Research Square

Preprints are preliminary reports that have not undergone peer review.
They should not be considered conclusive, used to inform clinical practice,
or referenced by the media as validated information.

First intravitreal mitochondrial transplantation for bilateral vision loss

David Putrino

david.putrino@mountsinai.org

Icahn School of Medicine at Mount Sinai

Christopher Kellner

Icahn School of Medicine at Mount Sinai

James McCully

Boston Children's Hospital

Gareth Lema

Icahn School of Medicine at Mount Sinai

Mansi Saxena

Icahn School of Medicine at Mount Sinai

Joshua Bederson

Icahn School of Medicine at Mount Sinai

Valerie Elmalem

Icahn School of Medicine at Mount Sinai

Melanie Walker

walkerm@uw.edu

University of Washington https://orcid.org/0000-0002-8995-4657

Case Report

Keywords: Mitochondrial transplantation, optic neuropathy, cerebral hypoperfusion, intravitreal injection, expanded access

Posted Date: August 10th, 2026

DOI: https://doi.org/10.21203/rs.3.rs-10622019/v1

License: This work is licensed under a Creative Commons Attribution 4.0 International License.
Read Full License

Additional Declarations: The authors declare potential competing interests as follows: Dr. Kellner directs research at Mount Sinai supported by funding from JNJ Medtech Neurovascular, Medtronic, Balt, Integra, Penumbra, Viz.AI, Siemens, Stryker, Longeviti, Irras, Clearpoint, ICE Neurosystems, Mobia, Kaneka, Terumo, Epic Neuro, EM Vision, Route92, and Precision Neuroscience; he has equity in Precision Recovery, Borealis, E8, Borvo, Periscope, Enso Vascular, and Metis Innovative. Metis Innovative is an investment group that has coordinated investments in Synchron, Proprio, Fluid Biomed, Von Vascular, Precision Recovery, Phantom Neuro, Radical, Aurenar, Reach Neuro, TET Medical, Enso Vascular, and Hyperion. The remaining authors declare no competing interests.

Abstract

Mitochondrial transplantation delivers viable, respiration-competent mitochondria into tissue whose own mitochondria have been damaged. It has been performed in the human heart and brain, but not in the eye, and no dose, safety profile or delivery experience existed for that compartment. Retinal ganglion cells depend heavily on oxidative phosphorylation, and in rodents mitochondria injected into the vitreous are taken up by these cells and improve survival after optic nerve injury. Here we show that fresh autologous mitochondria, isolated at the point of care, can be injected into the human vitreous without ocular or systemic toxicity. A 26-year-old woman with bilateral optic neuropathy fixed for three months after prolonged cerebral hypoperfusion received one injection into each eye, 24 hours apart, under emergency expanded access. Neither eye developed intraocular inflammation, and automated pupillary reactivity, absent across 45 readings over the preceding 71 days, returned in each eye within days of its own injection, transiently and without measurable acuity change.

Introduction

Mitochondrial transplantation is the delivery of viable, respiration-competent mitochondria into tissue whose own mitochondria have been damaged. Isolated mitochondria are internalized by host cells within minutes, largely by actin-dependent endocytosis (McCully et al. 2009; Pacak et al. 2015; Cowan et al. 2017; Doulamis and McCully 2021), paralleling the physiologic transfer of mitochondria from astrocytes to injured neurons after stroke (Hayakawa et al. 2016).

Human experience with the fresh autologous platform is confined to settings outside the eye. However, the therapeutic precedent for autologous mitochondrial transplantation in oxygen-depleted conditions has been established for recovery of ventricular function after congenital cardiac surgery (Emani et al. 2017; Guariento et al. 2021) and acceptable short-term safety during mechanical thrombectomy for large-vessel ischemic stroke (Walker et al. 2026). In both, the product was administered at or near the time of injury and the target organ was reached directly by open surgery or an intra-arterial catheter. This prior knowledge and experience were applied to a young female patient with nearly complete vision loss bilaterally due to a severe intracerebral hemorrhage caused by prolonged cerebral hypoperfusion, ischemic optic neuropathy, and traumatic optic neuropathy from both deceleration as the patient hit the ground and compression from prone position.

Autologous mitochondrial transplantation was chosen based on its direct mechanism of action within ischemic tissues, the ability to apply the mitochondria directly to the injured neurons, and the absence of any other effective treatment option. Based on these criteria and the severity of the patient’s vision loss, the treatment was given under the approval of an individual-patient emergency investigational new drug designation granted by the FDA.

The underlying injury was not a generic form of neuronal loss. In ischemia-reperfusion injury (IRI), the sequence leading to cell death converges on the mitochondrion. Oxygen deprivation depletes adenosine triphosphate and sodium-potassium ATPase-dependent ion homeostasis fails. On reperfusion, reactive

oxygen species are generated, mitochondrial membrane potential collapses, the permeability transition pore opens, and cytochrome c release initiates intrinsic apoptosis (Yoshida et al. 2024). Transplanted mitochondria restore bioenergetic capacity in injured but living cells; although they have not been shown to replace cells that have died (Brestoff et al. 2025).

Intravitreal injection was chosen as the safest and most direct route of administration. First and foremost, preclinical animal models have shown that mitochondria delivered into the rodent vitreous are taken up predominantly by the ganglion cell, inner plexiform, and inner nuclear layers (Cakir et al. 2026). In optic nerve crush, intravitreal delivery increased RGC survival, improved electrophysiological responses, and increased axonal regeneration beyond the crush site (Nascimento-dos-Santos et al. 2020). Intravitreal injection deposits the product against the inner retinal surface, where RGC somata and the nerve fiber layer supplying the optic nerve head are situated.

Alternative routes either lacked utility and/or posed unacceptable risks. Ophthalmic artery catheterization risks occlusion of the central retinal artery or terminal capillaries with a particulate suspension. Subretinal delivery requires a complex surgery and targets the outer retina, Suprachoroidal injection risks sheering the mitochondria and would not target the correct tissues. Finally, intravenous administration has no preclinical evidence of retinal delivery.

The retina is a plausible target on metabolic grounds. RGCs sustain among the highest energy demands in the central nervous system and depend on oxidative phosphorylation across a long unmyelinated intraretinal segment (Muench et al. 2021). Mitochondrial dysfunction is a common final pathway in optic neuropathies of otherwise unrelated cause, and both vulnerability and regenerative capacity are graded across RGC subtypes rather than uniform (Ou et al. 2016; Tao et al. 2019; Tapia et al. 2022).

Uptake after intravitreal delivery is enriched along nerve fiber bundles and extends along the proximal optic nerve over 24 hours, and the effect in optic nerve crush depends on organelle structural integrity (Cakir et al. 2026; Nascimento-dos-Santos et al. 2020). The same route attenuates retinal layer loss in retinal degeneration (Wu et al. 2022), restores respiratory chain function in inherited optic neuropathy (Wang et al. 2024), and rescues patient-derived neurons when targeted to cell type (Ayupov et al. 2026); in retinal pigment epithelial and ganglion precursor cells, exogenous mitochondria integrate into the host network and restore adenosine triphosphate production under oxidative stress (Aharoni-Simon et al. 2022; Noh et al. 2024).

The proposed mechanism is rescue rather than regeneration. Transplanted mitochondria restore bioenergetic capacity in injured but living cells; they have not been shown to, and are not proposed to, replace cells that have died (Brestoff et al. 2025). The intervention therefore has a substrate requirement, and its plausibility in a given patient depends on whether a compromised but viable population remains at the time of delivery. That question is empirical and can be addressed before treatment rather than inferred afterwards. Here, two pre-treatment findings bore on it: SSVEP indicated that afferent signal continued to reach visual cortex, and optical coherence tomography (OCT) showed nerve fiber and ganglion cell layer thinning rather than absence.

No mitochondrial product had previously been administered to the human eye, and no human dose, safety profile or delivery experience existed for this compartment. To the best of our knowledge, we report the first administration of a mitochondrial product to the human eye. This was undertaken with therapeutic intent under an individual-patient emergency investigational new drug application in a patient with severe fixed visual loss for which no established treatment exists. Identical injections were performed sequentially in each eye with prespecified tolerability gating between procedures. The outcomes reportable from a single case are feasibility, safety, and the temporal relationship between the procedures and objective measures of afferent visual function.

Results

Clinical course and substrate at the time of treatment

A previously healthy 26-year-old woman sustained a spontaneous left frontal intracerebral hemorrhage from a ruptured cerebral arteriovenous malformation. An estimated 18-hour pre-hospital interval produced sustained cerebral hypoperfusion with raised intracranial pressure. She was found face down with an abrasion of the right brow, indicating a fall and prolonged prone position. On arrival she had absent cranial nerve reflexes and no movement to noxious stimulus. She underwent emergent decompressive hemicraniectomy with clot evacuation, followed by definitive resection of the malformation. Residual neurological deficits were expressive aphasia and right hemibody weakness. The course is shown in Fig. 1.

The initial ophthalmic exam found the right pupil to be minimally reactive and the left to be unreactive to direct light; the fundus was normal without papilledema. Automated pupillometry on the same day was concordant, with no measurable response in the right eye across 11 readings and the only measurable values in the left. Contributing mechanisms to the visual loss were prolonged dependent prone positioning affecting optic nerve perfusion, a protracted period of raised intracranial pressure transmitted to the optic nerves through the perineural subarachnoid space, and traumatic optic neuropathy from a fall onto the right side of the face. Examination at 8 weeks showed bilateral optic disc pallor and atrophy. The differential was narrowed as follows. A compressive or structural cause was excluded by magnetic resonance imaging, which showed volume loss of the optic chiasm and prechiasmatic optic nerves without a mass, hematoma or other compressive lesion. Inflammatory and demyelinating optic neuropathy was excluded by the absence of active T2 or fluid-attenuated inversion recovery signal change or enhancement in the optic nerves, and by the absence of pain on eye movement. Infiltrative and infectious causes were excluded on the same imaging, which showed no optic nerve or leptomeningeal enhancement, together with the absence of systemic features. A retinal cause, including central retinal and ophthalmic artery occlusion, was excluded by a normal acute fundus examination without inner retinal opacification and by optical coherence tomography showing normal outer retinal and foveal morphology. A post-geniculate cause was excluded by the pupillary findings themselves, since the pupillary light reflex is spared in cortical blindness. Leber hereditary optic neuropathy, which can present with bilateral visual loss in this age group, was considered improbable

given the abrupt onset coincident with a documented period of hypoperfusion and the absence of family history; genetic testing was not performed. Toxic and nutritional causes were excluded by the abrupt onset coincident with a documented period of hypoperfusion, which is incompatible with the slowly progressive bilateral central visual loss that characterizes them. The presentation was attributed to combined ischemic and traumatic optic neuropathy.

Imaging also showed a mature left frontal postoperative cavity with limited surrounding gliosis, with intact occipital cortex bilaterally (Fig. 2a to c).

Fundus imaging prior to the procedure was limited by the patient's inability to position at the scanner, and only single optical coherence tomography (OCT) scans were obtained. These showed normal outer retinal and foveal morphology with severe thinning of the nerve fiber layer and ganglion cell layer in both eyes (Fig. 2d). Fundus photography obtained with a RetCam at the time of treatment showed optic nerve pallor in both eyes (Fig. 2e).

Before treatment, best-corrected acuity was intermittent, questionable light perception in the right eye and light perception in the left, with no pupillary response on the right and a slight response on the left, concordant with the automated pupillometry over the same interval. The visual deficit had been fixed for approximately 3 months at the time of treatment.

Product manufacture and release

Two manufacturing events were performed, one for each eye. Both products met all pre-release acceptance criteria: no gross aggregates, fibers or particulates on visual inspection; endotoxin below 0.5 EU/mL; and no organisms on Gram stain. Hemocytometer counts gave 7.5 x 10^7 mitochondria for the first product, administered to the right eye, and 2.5 x 10^7 for the second, administered to the left. Both were released and administered within the specified hold window. Post-administration testing per United States Pharmacopeia General Chap. 71 showed no growth at 7 and at 14 days for both products. No stop rule was met and no deviation required product disposition.

Safety

Both injections were well tolerated, with no serious adverse event. There was no rise in intraocular pressure, no intraocular inflammation, no endophthalmitis and no traction retinal detachment. All permissive criteria for contralateral eye treatment were met at the 24-to-36-hour assessment and no prohibitive criterion was present. Inflammatory and immune surveillance remained within reference intervals at every timepoint through 4 weeks (Table 2).

Table 2
Inflammatory and immune surveillance before and after treatment.

Test	Reference range	Baseline	24 h	Days 2 to 5	4 weeks
Interleukin-6 (pg/mL)	not more than 7	4.2	1.4	5.6	2.1
Tumor necrosis factor alpha (pg/mL)	0 to 22	12	10	11.6	8.1
C-reactive protein (mg/L)	less than 3.0	less than 3.0	less than 3.0	less than 3.0	less than 3.0
Ferritin (ng/mL)	12 to 307	32	33	36	33
Total hemolytic complement CH50 (U/mL)	52 to 95	56	NA	57	56
Complement C3 (mg/dL)	90 to 180	133	NA	137	113
Complement C4 (mg/dL)	15 to 45	37	NA	35	30
Anti-mitochondrial DNA antibody	less than 20	less than 20	NA	less than 20	less than 20

*No analyte moved outside its reference interval at any timepoint. NA indicates not assayed.

Pupillary reactivity before and after treatment

Automated pupillometry comprised 239 readings over 141 days, 121 in the right eye and 118 in the left. Sampling was intermittent and clinically determined and included a 52-day interval during inpatient rehabilitation from which no readings are available (Fig. 1). The pre-treatment record therefore comprises two intervals that should not be pooled. All five pre-treatment readings meeting the criterion for a normal light reaction, defined a priori as a Neurological Pupil index (NPi) of at least 3.0, occurred in the first 24 days after the hemorrhage, three of them within the first 2 days. Each of those five was an isolated reading: on each occasion the same eye was sampled 3 to 15 times that day and every other reading fell below the criterion, most at or near zero. In the 71 days immediately preceding treatment there were 45 readings, 23 in the right eye on 7 sampling days and 22 in the left on 6 sampling days, and none met the criterion; the maximum index in that interval was 1.3 on the right and 2.5 on the left. The last reading obtained in each eye before its own procedure fell within the preceding 24 hours and did not meet the criterion.

Against this fixed baseline, the proportion of readings meeting the criterion after treatment was 6 of 28 in the right eye (21.4 percent, 95 percent Wilson interval 10.2 to 39.5) and 7 of 24 in the left (29.2 percent, 14.9 to 49.2), giving Fisher exact p = 0.027 and p = 0.010 respectively and p = 0.00015 for the two eyes combined (0 of 45 against 13 of 52) (Fig. 3b, Table 1). A day-block bootstrap resampling whole days gave an increase of 21.4 percentage points in the right eye (95 percent interval 7.4 to 37.5) and

29.2 points in the left (12.5 to 47.8). A beta-binomial model with a uniform prior gave a posterior probability that the post-treatment fraction exceeded the baseline fraction of 0.990 for the right eye and 0.997 for the left.

Table 1
Pupillary reactivity by interval and comparison against the fixed pre-treatment baseline.

Interval	Right eye	Left eye
Acute period, more than 71 days before treatment	3/70 (4.3)	2/72 (2.8)
Fixed baseline, 71 days before treatment	0/23 (0)	0/22 (0)
Days 1 to 14 after treatment	4/16 (25.0)	7/12 (58.3)
Days 15 to 28 after treatment	1/4 (25.0)	0/4 (0)
Day 29 onward	1/8 (12.5)	0/8 (0)
All readings after treatment	6/28 (21.4)	7/24 (29.2)
Fisher exact p, after treatment against fixed baseline	0.027	0.010
Day-block bootstrap difference, percentage points (95%)	+ 21.4 (7.4 to 37.5)	+ 29.2 (12.5 to 47.8)
Beta-binomial posterior P(after > baseline)	0.990	0.997
First reading meeting criterion after treatment	day 4	day 2
Peak index after treatment (day)	4.4 (day 4)	4.1 (day 4)
Last reading meeting criterion	day 39	day 11
Maximum index during fixed baseline	1.3	2.5

**Values are readings meeting the criterion for a normal light reaction, defined as Neurological Pupil index of at least 3.0, over readings obtained, with percentage in parentheses. Intervals are measured from each eye's own procedure. The acute period and the fixed baseline are reported separately and are not pooled. Fisher exact p for the two eyes combined, 0 of 45 against 13 of 52, is 0.00015.*

Each eye met the criterion within days of its own procedure. Onset was on day 4 in the right eye and on day 2 in the left, with peak values of 4.4 and 4.1, both on day 4 (Fig. 3a). The order of onset did not follow the order of treatment: the left eye, treated second, was the first to meet the criterion.

Trajectory and durability

Reactive rates by epoch, with Wilson intervals, are given in Table 1 and Fig. 3c. The rate peaked on days 1 to 14 in both eyes, at 25.0 percent (10.2 to 49.5) in the right eye and 58.3 percent (32.0 to 80.7) in the left and fell thereafter. Denominators in the later epochs are small.

The two eyes differed in pattern. In the left eye, 7 of the 8 days sampled between day 2 and day 11 met the criterion, and none of the 12 days sampled thereafter did; the last was day 11. In the right eye, 6 of 22 sampled days met the criterion, distributed across days 4, 5, 6, 12, 19 and 39, with a longest run of 3 consecutive sampled days. Neither eye established a new sustained baseline: from day 29 onward the mean index was 1.15 in the right eye against 0.70 in the fixed baseline, and 0.83 in the left against 1.07.

Between-eye relationship and confound checks

Correlation between simultaneous readings from the two eyes fell after treatment, from a Spearman coefficient of 0.66 across 94 paired pre-treatment readings (95 percent interval 0.53 to 0.76) to 0.14 across 24 paired post-treatment readings (-0.28 to 0.52), a difference of z = 2.68, p = 0.007. On 7 of the 10 post-treatment days on which either eye met the criterion, only one eye did so, and the two eyes met it on the same day on 3 occasions. Reactivity was not associated with time of day in either eye (p = 0.67 for both). Repeat scans within a single session varied by a median of 0.21 index units in the right eye and 0.28 in the left before treatment, which bounds short-term measurement variation; after treatment the corresponding medians were 1.06 and 1.36, and the standard deviation of all readings rose from 0.77 to 1.38 in the right eye (Levene p = 0.003) and from 0.78 to 1.45 in the left (p < 0.001).

Determinants of the pupillometry index in this patient

Eight-parameter device captures were retained from the day of the second procedure onward and were available for 40 captures, of which 36 had a complete component vector; the remaining 4 recorded no measurable constriction (Fig. 4a). Across these, NPi was almost entirely reconstructed from two of the eight displayed parameters. A two-term model using resting pupil diameter and percentage constriction explained 93 percent of the variance (NPi = 4.53 + 0.103 x constriction in percent − 0.775 x size in mm; R-squared 0.927, cross-validated 0.910); adding the other four parameters raised R-squared to 0.945 and none was significant. The two retained terms were significant and of opposite sign, each millimeter of resting diameter lowering the index by 0.775 points at fixed constriction (p = 2.4 x 10^-14) and each percentage point of constriction raising it by 0.103 points (p = 4.5 x 10^-9), so that approximately 7.5 percentage points of additional constriction were required to offset each millimeter of resting dilation. Partial correlations, standardized coefficients, random forest importances and the full model comparison are given in Supplementary Table 1.

Across the 9 captures meeting an independent criterion for a measured reflex, defined as constriction of at least 10 percent, the index was ordered by resting diameter rather than by constriction (Spearman −0.895 against size, p = 0.001; +0.228 against constriction, p = 0.56). Every such capture at a resting diameter of 2.47 to 3.99 mm scored 3.3 to 4.4, and every one at 4.81 to 5.88 mm scored 1.4 to 1.6, despite equal or greater constriction (Fig. 4b). The index was uncorrelated with average constriction velocity across these captures (Pearson r = 0.001), and classifying each capture independently by the two gave discordant results in 14 of 36. Resting diameter set the direction: captures called normal by

index but sluggish by velocity had diameters of 2.47 to 3.99 mm and those called abnormal by index but brisk by velocity had diameters of 4.81 to 5.88 mm, with no overlap (p = 0.002, Supplementary Table 2).

Because the index is dominated by resting diameter, whether the post-treatment readings reflected greater constriction or only smaller resting pupils was examined directly in the component data. Captures meeting the criterion had both smaller resting pupils and larger constriction than those that did not: in the right eye, mean constriction was 14.8 percent against 3.8 percent (p = 0.008) and absolute constriction 0.45 mm against 0.21 mm (p = 0.028); in the left eye, mean constriction was 11.3 percent against 6.0 percent (p = 0.039), with absolute constriction 0.39 mm against 0.33 mm (p = 0.47) (Fig. 4c). Because component data are available only from the treatment period onward, this comparison is between captures within that period and not between periods.

Cortical responses

SSVEP were recorded at 5 sessions, 2 before treatment and 3 after, yielding 7 captures. Neither pre-treatment session showed an organized multi-channel response. At 27 days before treatment the response was confined to O1, with O2 and Oz near the noise floor. At 4 days before treatment, the session nearest the procedure, all three channels were at globally low amplitude with a borderline response and no clear dominant channel.

An organized occipital response involving O2 and Oz was present at all three post-treatment sessions, on days 3, 44 and 45: initially with O1 and O2 comparable across a 5 to 16 Hz band, then with the three channels overlapping, and at the final session with O1 at the noise floor and O2 and Oz showing the response. No recording was obtained between day 3 and day 44, so the finding is that an organized response was present whenever it was sought after treatment and at neither session before it, not that it was continuously present. Single-eye stimulation at day 45 produced an O2-dominant response on left-eye stimulation and an Oz-dominant response on right-eye stimulation. Session-level detail is given in Supplementary Table 7. Two of the seven captures have an archived device screen image, the pre-treatment session 4 days before the first procedure and the first post-treatment session 3 days after it; both are provided with Supplementary Data 1, and the remaining sessions are recorded in the contemporaneous session log only.

Visual acuity

Measurable visual acuity did not change. Light perception in the right eye was recorded before treatment as intermittent and questionable and afterwards as consistent, and the left eye had light perception before and after. A formal low vision assessment 2 weeks after both injections recorded bare light perception at best in the right eye, and light perception with a constricted visual field in the left, the field being slightly larger superotemporally than nasally or inferotemporally. The treating ophthalmologists additionally observed that the patient began to reach for specific objects after treatment, which had not been observed before. This was an unblinded bedside observation, was not quantified, and was not

accompanied by a measurable change in acuity; reaching also requires motor, attentional and cognitive function, all of which were recovering over the same interval.

Discussion

To our knowledge, this is the first administration of isolated mitochondria to the human eye. The procedure was performed to the filed specification in both eyes, both products met release criteria, and neither eye developed intraocular inflammation, raised pressure, endophthalmitis or retinal detachment. Systemic inflammatory and immune surveillance was unchanged throughout. The principal theoretical hazard of placing a particulate biological suspension into a closed, immune-privileged compartment is sterile inflammation mediated by damage-associated molecular patterns. No such signal was observed with a fresh autologous product, which is the observation of most immediate use to anyone considering this route.

Objective functional changes followed the procedures, and four features of their pattern constrain the possible explanations. The immediate pre-treatment baseline was fixed: across 45 readings in the 71 days before treatment neither eye produced a normal light reaction, and the last reading in each eye, obtained within 24 hours of its own procedure, did not either. Each eye then met the criterion within 2 to 4 days of its own injection. The eyes decoupled, with correlation between simultaneous readings falling from 0.66 to 0.14 and only one eye meeting the criterion on 6 of the 9 days on which both were sampled and either did. And the component data show that the readings meeting the criterion showed genuinely larger constriction, not only smaller resting pupils, which matters because the index itself is dominated by resting diameter.

The pre-treatment record contains two intervals that should not be pooled. Five readings met the criterion in the first 24 days after the hemorrhage, three of them in the first 2 days. Variability of this kind early after acute brain injury is expected and well described: in the ORANGE cohort, the largest prospective series of automated pupillometry in acute brain injury, NPi values varied within and between patients during the first week, and it is repeated abnormality rather than any individual reading that has prognostic weight (Oddo et al. 2023). ORANGE characterizes the first week and so speaks to three of these five readings; the remaining two fall at 23 and 24 days, within the interval in which spontaneous improvement after ischemic optic neuropathy is itself described. The interval that anchors the present comparison is neither of these but the 71 days that followed, during which the deficit was fixed and none of 45 readings in either eye met the criterion.

A shared driver, whether spontaneous recovery, fluctuating arousal, or a systemic effect of concurrent therapy, predicts that the eyes move together, and they did not. The concurrent therapies, red and near-infrared light, a microtesla magnetic-field system and memantine, were begun before the first injection and were bilateral or systemic and continuous, and so do not predict eye-specific, injection-timed change. Reactivity was unrelated to time of day. Repeat scans within a session varied by about 0.2 to 0.3

index units before treatment, so the post-treatment peaks of 4.4 and 4.1, against a 71-day baseline maximum of 1.3 and 2.5, are not attributable to short-term measurement variation.

Spontaneous visual improvement after ischemic optic neuropathy is well described, occurring in 38 of 89 eyes followed without intervention in the Ischemic Optic Neuropathy Decompression Trial and in some untreated cases in the largest reported posterior ischemic optic neuropathy series (Ischemic Optic Neuropathy Decompression Trial Research Group 1995; Hayreh 2004). It is, however, an acute and subacute phenomenon: visual function typically stabilizes by approximately 2 months, coincident with the replacement of disc edema by optic atrophy, and change beyond that point is atypical. In this patient optic atrophy was documented at 8 weeks and the deficit was fixed across the subsequent 71 days. Improvement first appearing at that stage is not a described feature of the natural history, and we identified no report of spontaneous return of pupillary reactivity in an optic neuropathy of comparable severity and chronicity.

A response approximately 3 months after injury requires that a viable population remained at the time of delivery, and RGC loss after ischemia is not instantaneous. In rodent models of pressure-induced retinal ischemia, ganglion cell death is an ongoing process whose severity and duration scale with the length of the insult and continue over weeks rather than completing at reperfusion (Selles-Navarro et al. 1996; Lafuente et al. 2002), human induced pluripotent stem cell-derived RGCs subjected to hypoxia-reoxygenation show graded rather than all-or-none injury (Yoshida et al. 2024), and a window during which dying ganglion cells remain rescuable has been described directly (You et al. 2024). Structure and function dissociated here as that account predicts: imaging showed fixed thinning of the nerve fiber and ganglion cell layers while the functional measures changed, which is consistent with rescue of residual function rather than structural regeneration.

That pupillary reactivity returned while measurable acuity did not is not itself unexpected: the severity of a pupillary defect corresponds more closely to the extent of visual field loss than to acuity (Thompson et al. 1982), and intrinsically photosensitive RGCs, which mediate the pupillary light reflex, are comparatively resistant to injury and are distinct from the population subserving image-forming vision (Cui et al. 2015; Tapia et al. 2022).

The response was not durable. Both eyes returned toward their pre-treatment state, the left, which had responded more persistently over the first 11 days, more completely than the right. One interpretation is substrate-dependent consolidation failure, in which a single dose restores bioenergetic capacity transiently in cells that cannot sustain it without continued support. On that reading, dose, interval and repetition become the operative variables, and the transience is a property of the schedule rather than of the approach. The present data cannot separate that from the alternative that the changes were unrelated to treatment.

Characterization of NPi in this patient bears on how the index should be used. Because the algorithm is proprietary, the weighting of the displayed components cannot be inspected and has to be recovered empirically. That the index is not independent of those components is established across 27,462

readings (Shoyombo et al. 2018); what the present case adds is the magnitude of that dependence within a single patient and its consequence for the clinical call. Across captures meeting an independent criterion for a measured reflex, the dependence inverted the reading, equal or greater constriction scoring in the normal range at small resting diameters and sluggish at large ones, and the index and average constriction velocity, the two numbers a clinician sees together, disagreed on 14 of 36 captures. The consequence is not that the index is noisier when the pupil is dilated but that it is biased, under-reporting a given reflex at large resting diameters and over-reporting it at small ones, in a direction predictable from the diameter alone. Where resting pupil size fluctuates, as it did here, the index and its components should be reported together, as they were throughout.

Sampling was clinically determined rather than scheduled. The 71-day fixed baseline comprises 45 readings obtained on 7 and 6 sampling days in the right and left eyes, with a 52-day interval during inpatient rehabilitation from which no readings exist, so it establishes that no normal light reaction was recorded whenever the eye was examined rather than continuous absence. For the same reason a data-driven change-point analysis is uninformative about onset timing beyond what the observation schedule already fixes, and it is reported in Supplementary Table 3 rather than as support here. The two eyes were treated 24 hours apart, so their courses are not fully independent, and the order in which they met the criterion was the reverse of the order of treatment. Denominators in the later epochs are small.

Attribution of the pupillary change to a specific RGC subtype was not possible, because chromatic pupillometry was not used and the device employed a white light stimulus (Rukmini et al. 2019); the subtype-specific account offered above is a hypothesis consistent with the observations rather than a finding. Eight-parameter component data were retained only from the day of the second procedure onward, so the index decomposition characterizes the measurement within the treatment period and cannot be extended backwards to the baseline.

Serial OCT with normative comparison could not be obtained because the patient could not reliably position at the scanner. SSVEP records exist only as photographs of automatically scaled device output with no numeric export, so no amplitude comparison is possible, sessions were widely spaced, and no monocular pre-treatment recording exists. Neuro-ophthalmological assessment was limited throughout by expressive aphasia and by acuity at the level of light perception.

Two manufacturing limitations bear on interpretation. Mitochondrial number was determined by hemocytometer rather than by particle counting, which may yield lower counts of the same preparation (Preble et al. 2014). Release was gated on four tests, comprising visual inspection for aggregates and particulates, identity and count, kinetic chromogenic limulus amoebocyte lysate endotoxin testing against a specification of not more than 0.5 EU/mL, and Gram stain, and both products met all four. The Gram stain was nonetheless the only rapid microbiological test available within the procedural window, and its detection threshold is approximately 10^4 to 10^5 colony-forming units per milliliter; compendial sterility testing by General Chap. 71 was negative for both products but available only after administration.

The observation that the patient began to reach for specific objects is the least able to bear weight of any reported here: it was unblinded, unquantified, and confounded by concurrent neurological recovery. No instrument suitable for a patient at the level of light perception with expressive aphasia was available to test it formally. Finally, treatment occurred late in the patient's recovery. Since mitochondrial transplantation depends on functional cells as the substrate, the severity of the injury and the prolonged interval before treatment likely limited the potential for visual recovery.

Intravitreal administration of fresh autologous mitochondria was feasible, was performed to specification, and was tolerated without ocular or systemic toxicity. The timing and eye-specificity of the objective functional changes that followed are directionally consistent with a treatment effect in a deficit that had been fixed for 3 months, and we identified no alternative explanation that accounts for the full pattern. The changes were transient, measurable acuity did not improve, and the outcome measures are surrogate, since pupillary reactivity and cortical evoked responses are not vision. A single patient without a comparator cannot establish causation. The findings identify the questions a controlled evaluation should address: dose, interval, repetition, and selection of patients with preserved substrate.

Methods

Regulatory framework and consent

Treatment was provided under an individual-patient expanded access investigational new drug application for emergency use, submitted under 21 CFR 312.310(d) with Form FDA 3926. The request was made on 7 May 2026 and the Center for Biologics Evaluation and Research granted emergency administration on 9 May 2026 under IND 32909, for the single-patient treatment of posterior ischemic optic neuropathy with autologous skeletal muscle mitochondria, with Christopher P. Kellner as sponsor-investigator. Expedited Institutional Review Board Chairperson concurrence was obtained before treatment, and the emergency use was reported to the Board within five working days, as required by 21 CFR 56.104(c). Written informed consent was obtained from the patient's legally authorized representative under 21 CFR 50.20, in compliance with the principles of the Declaration of Helsinki; the exception from informed consent requirements at 21 CFR 50.23 was therefore not invoked. Manufacture, release testing and administration followed a standard operating procedure filed with the application. The product was manufactured under the Phase 1 investigational drug exemption at 21 CFR 210.2(c) and the framework described in the FDA guidance on chemistry, manufacturing and controls flexibilities for cellular and gene therapy products (FDA 2026). Adverse events were captured per 21 CFR 312.32. Family, psychosocial and lifestyle history are not reported, and calendar dates are replaced throughout by intervals and study days, to protect the identity of a single identifiable patient. The patient's own perspective on treatment could not be obtained because of expressive aphasia; her legally authorized representative provided consent, was consulted throughout, and reviewed this report.

Drug product

The product was a suspension of fresh autologous mitochondria isolated at the point of care. It was not cultured, expanded, genetically modified, cryopreserved or frozen at any point. Source tissue was obtained under general anesthesia by 6 mm biopsy of the vastus medialis, yielding approximately 100 mg, and transported on ice in sterile saline to the institutional cGMP facility. A second biopsy was taken from the contralateral leg at the time of the second procedure.

Isolation followed the tissue dissociation and differential filtration method of Preble et al. (2014) as subsequently described by Doulamis and McCully (2021). Tissue was washed twice in sterile saline, homogenized in cold Solution A using a Miltenyi tissue dissociator on the standardized h-mitochondria program, digested with subtilisin A for 10 minutes at 4 degrees C, and passed sequentially through two 40 micrometer and one 10 micrometer filters. The filtrate was pelleted at 9,500 rpm for 5 minutes at 4 degrees C and washed three times in cold Solution A at 14,000 rpm for 5 minutes at 4 degrees C. The final pellet was resuspended in approximately 100 microliters of cold Solution A to a working concentration of approximately 2 x 10^9 mitochondria per mL, the additional volume accounting for syringe and needle dead space. Solution A comprised 300 mM sucrose, 10 mM potassium HEPES at pH 7.2 and 1 mM potassium EGTA at pH 8.0, filter sterilized through a 0.22 micrometer unit. This vehicle was used in preference to respiration medium, which requires fresh preparation and additional steps to assure sterility within the procedural window (Doulamis and McCully 2021).

Isolation and dispensation were performed in an ISO 5 biological safety cabinet within an ISO 7 non-viral cleanroom, with pre- and post-production environmental monitoring by active air sampling, non-viable particle counting, settling plates and operator glove-point touch plates. Isolation was performed by the developer of the methodology under the direction of the sponsor-investigator, with an institutional quality assurance specialist present as observer and verifier. Manufacturing was documented contemporaneously on a log recording reagent lots, equipment, personnel and timings for each critical step, in-process observations, release results, and times of resuspension, release, transport and administration.

Release testing, product hold and stability

Mitochondria of 0.5 to 1.5 micrometers fall within the size class retained by 0.22 micrometer sterilizing-grade filters, so terminal sterilization by membrane filtration was not possible. Sterility assurance therefore depended on aseptic process control, sterile-filtered buffers and consumables, and the testing scheme below.

Four tests gated release. Visual inspection required a clear to slightly turbid suspension with no gross aggregates, fibers or particulates. Identity and quantity were determined by MitoTracker Orange CMTMRos labeling with hemocytometer counting. Endotoxin was measured on the final formulated product by kinetic chromogenic limulus amoebocyte lysate assay using an FDA-licensed Endosafe nexgen-PTS cartridge system per United States Pharmacopeia General Chap. 85, with a specification of not more than 0.5 EU/mL and not more than 2.0 EU per dose per General Chap. 771; each cartridge

performed duplicate testing with a positive product control and spike recovery within a 50 to 200 percent window, with a cycle time of approximately 15 minutes. At a 50 microliter volume the per-dose limit corresponds to 40 EU/mL, so the per-mL limit was binding, and the cartridge range of 0.005 to 10 EU/mL sits within it. Rapid microbial detection was by STAT Gram stain on an approximately 100 microliter retention aliquot, specification no organisms observed, cycle time approximately 15 to 20 minutes. Compendial sterility testing by General Chap. 71 direct inoculation into fluid thioglycollate and soybean-casein digest media was performed on a separate retention aliquot taken before administration; results become available only after administration.

Hold time from completion of resuspension to completion of administration was documented, target not more than 60 minutes and absolute maximum 120 minutes. During the hold window the product was maintained at 4 degrees C in a sealed sterile container, and in an insulated container with cold-pack temperature control during transfer to the operating room. These limits follow published stability data for mitochondria isolated by this method and held on ice in Solution A, in which oxygen consumption rate did not differ significantly from baseline at 30, 60, 90 or 120 minutes after isolation (101.6, 94.3, 91.3 and 94.6 nM O2 per minute per mg mitochondrial protein) and declined significantly by 180 minutes (McCully et al. 2023).

Administration

Procedures were performed in the operating room under general anesthesia, required because expressive aphasia precluded cooperation with awake injection. Technique followed the consensus guidelines of Avery et al. (2014). Oral moxifloxacin 400 mg every 24 hours was started 24 to 48 hours beforehand (Hariprasad et al. 2006). Isolation was performed in parallel during procedural setup, and the released product was transported under chain of custody with receipt verified before injection.

Examination under anesthesia comprised anterior chamber assessment, pupil reactivity, indirect ophthalmoscopy and tonometry. Antisepsis was performed in two stages, 10 percent povidone-iodine to the periocular skin, then a sterile wire lid speculum and 1 to 2 drops of 5 percent povidone-iodine ophthalmic solution to the ocular surface with at least 30 to 60 seconds of contact. The injection site was marked at the superotemporal pars plana 4 mm posterior to the limbus by scleral indentation with sterile calipers. An anterior chamber paracentesis was performed through the temporal cornea with a 30-gauge needle and 0.1 mL of aqueous withdrawn before injection, to accommodate the injected volume and limit the rise in intraocular pressure. Fifty microliters of the released suspension in Solution A was injected into the vitreous cavity through the marked site using a 30-gauge half-inch needle on a 1 mL Luer-Lock tuberculin syringe, approximately 100 microliters having been drawn up with the residual retained in dead space. The injection volume was prespecified in the filed protocol; the number of mitochondria delivered was determined by the yield of each isolation.

After injection, optic nerve perfusion was confirmed by indirect ophthalmoscopy and intraocular pressure measured, with repeat paracentesis planned if pressure exceeded 40 mmHg or perfusion was

poor. The patient was positioned supine for 20 minutes to allow settling of the suspension onto the posterior pole and optic nerve head, with tonometry at 10 minute intervals. Residual povidone-iodine was rinsed and topical neomycin-polymyxin-dexamethasone applied and continued afterwards. Empirical endophthalmitis treatment readiness was maintained throughout, with intravitreal vancomycin 1 mg in 0.1 mL, ceftazidime 2.25 mg in 0.1 mL and voriconazole 100 micrograms in 0.1 mL prepared on standby and pars plana vitrectomy available on site (Endophthalmitis Vitrectomy Study Group 1995; Hariprasad et al. 2004; Durand 2017).

Administration followed a prespecified sequential single-eye design with one dose per eye. The right eye, identified on pre-procedure imaging triage as having the comparatively worse substrate, was treated first. Treatment of the contralateral eye was gated by a go or no-go assessment between 24 and 36 hours against five prespecified permissive criteria (preserved light perception and no new relative afferent pupillary defect in the treated eye, intraocular pressure between 6 and 25 mmHg, absence of endophthalmitis signs, absence of rhegmatogenous retinal detachment, and absence of new retinal vascular sheathing, non-perfusion, hemorrhage or occlusive vasculitis) and eight prohibitive criteria, all of which had to be absent. Stop rules were prespecified: the intervention was not to proceed, or not to be repeated in the contralateral eye, in the event of failure of any pre-release test, hold time exceeding 120 minutes, clinical evidence of endophthalmitis, retinal detachment, retinal vasculitis or refractory intraocular pressure elevation in the first eye, or any serious adverse event judged to indicate unacceptable risk.

Assessments

Automated pupillometry used the NeurOptics NPi-200, which reports NPi together with resting and minimum pupil diameter, percentage constriction, average and maximum constriction velocity, latency and dilation velocity. NPi is a single scalar derived by a proprietary algorithm from the pupillary light reflex and scored against a normative reference set of more than 600,000 normal reflexes; the algorithm and its weighting of the displayed components are not disclosed (Chen et al. 2011; NICE 2020). It has been validated against outcome in the largest prospective multicentre cohort of automated pupillometry in acute brain injury (Oddo et al. 2023). Readings were obtained intermittently as clinically feasible from admission to the end of follow-up and were transcribed from the device record. No data were imputed; intervals without readings, including the 52-day interval during inpatient rehabilitation, reflect absence of assessment rather than missing values. Eight-parameter captures were retained from the day of the second procedure onward; earlier records comprise the index only.

SSVEP were recorded from occipital channels O1, O2 and Oz. Records exist only as photographic captures of the device frequency-domain output, with no numeric export, and archived images survive for two of the seven captures. Within a plot the three channel traces are overlaid rather than offset, so relative channel amplitudes are approximate. Device plots are automatically scaled, full-scale values ranging from 0.6 to 10 microvolts across sessions, so absolute amplitudes cannot be compared

between sessions; analysis was restricted to within-session channel topography, peak frequency band, and presence or absence of an organized response, which was defined as concordant peaks above the plotted noise floor in at least two occipital channels within a common frequency band. All sessions were binocular except two single-eye captures at the final session.

Additional assessments comprised OCT (Heidelberg Engineering), fundus photography (RetCam) and serial ophthalmologic examination. Inflammatory and immune surveillance comprised interleukin-6, tumor necrosis factor alpha, C-reactive protein, ferritin, complement CH50, C3 and C4, and anti-mitochondrial DNA antibodies at baseline, 24 hours, days 2 to 5 and 4 weeks, matching the immune endpoints reported for this platform (Ramirez-Barbieri et al. 2019). The patient received concurrent therapies begun before the first injection and continued throughout: red and near-infrared light, a microtesla magnetic-field system, and memantine. All were bilateral or systemic and continuous.

Statistical analysis

All analyses were within-patient and were performed in Python 3 using statsmodels, scikit-learn and SciPy. A normal pupil reaction, per standard, was defined a priori as NPi of at least 3.0. Time was measured from each eye's own procedure. No sample size or power calculation applies. Reported intervals are 95 percent intervals presented descriptively, and no adjustment for multiplicity was prespecified or applied.

The comparison designated as primary was the proportion of readings meeting the criterion in the 71 days immediately preceding each eye's procedure against the proportion after it, by Fisher exact test. That window was chosen because it begins after the last pre-treatment reading meeting the criterion and coincides with the interval over which the clinical deficit was documented as fixed; the earlier acute period is reported separately and not pooled with it. Supporting analyses were a day-block bootstrap resampling whole days with 20,000 replicates, a beta-binomial model with a uniform Beta(1,1) prior, and reactive rates by epoch with Wilson intervals using prespecified epoch boundaries. Between-eye dependence was assessed by Spearman correlation of readings acquired at the same timepoint before and after treatment, compared by Fisher z transformation, and by counting days on which only one eye met the criterion. Prespecified confound checks comprised logistic regression of reactivity on time of day, the within-session dispersion across repeat scans as an estimate of measurement variation, and comparison of dispersion before and after treatment by Levene test.

Because NPi is a composite index, its dependence on the displayed components was characterized in this patient before it was used as an outcome. Complete-case device captures were regressed on the displayed components by ordinary least squares, ridge regression and random forest, with leave-one-out cross-validation and day-clustered standard errors, and partial correlations were computed for each retained term. Component values were compared between captures above and below the index criterion by Mann-Whitney test. A data-driven single-split change-point analysis was performed and is reported in

Supplementary Table 3 with its profile-likelihood support interval; because the support interval extends across the unobserved interval before treatment, it is not used as evidence of onset timing.

Declarations

Competing interests

Dr. Kellner directs research at Mount Sinai supported by funding from JNJ Medtech Neurovascular, Medtronic, Balt, Integra, Penumbra, Viz.AI, Siemens, Stryker, Longeviti, Irras, Clearpoint, ICE Neurosystems, Mobia, Kaneka, Terumo, Epic Neuro, EM Vision, Route92, and Precision Neuroscience; he has equity in Precision Recovery, Borealis, E8, Borvo, Periscope, Enso Vascular, and Metis Innovative. Metis Innovative is an investment group that has coordinated investments in Synchron, Proprio, Fluid Biomed, Von Vascular, Precision Recovery, Phantom Neuro, Radical, Aurenar, Reach Neuro, TET Medical, Enso Vascular, and Hyperion. The remaining authors declare no competing interests.

Funding

This research received no specific grant from any funding agency in the public, commercial or not-for-profit sectors.

Author contributions

D.P. originated the concept of applying mitochondrial transplantation to this indication and coordinated the program. C.P.K. held the investigational new drug application as sponsor-investigator, was responsible for all communication with the Food and Drug Administration, and performed the source tissue biopsies. J.D.M. developed the isolation methodology and isolated the mitochondria for both procedures. M.S. directed the cGMP facility and managed quality assurance for manufacture and release testing. G.M.C.L. performed both intravitreal administrations and follow up ocular imaging. V.I.E. provided neuro-ophthalmological care and performed the clinical assessments before and after treatment. J.B.B. provided departmental oversight and institutional support for the program. M.W. prepared the clinical treatment protocol, designed and performed analyses, wrote the analysis code, produced the figures, and drafted the manuscript. D.P., C.P.K. and M.W. contributed equally. All authors reviewed and approved the manuscript.

Acknowledgements

We thank Bill Ackman, Karen Herskovitz and Lucy Ackman for their support and their commitment to advancing scientific discovery. We thank Spencer Lorin, Clinical Research Coordinator in the Department

of Neurosurgery, Icahn School of Medicine at Mount Sinai, for assistance in sourcing and de-identifying patient images.

Data availability

The de-identified pupillometry and evoked potential data supporting the findings are provided as Supplementary Data 1, a single workbook comprising the full index series, the source-of-record capture table with per-capture provenance, and the session register. Calendar dates are replaced by study days, and no patient, device or operator identifier is included.

Code availability

All analyses and figures were generated by custom Python code, provided as Supplementary Software, which reproduces every reported statistic from Supplementary Data 1. The code is archived at Zenodo under https://doi.org/10.5281/zenodo.21746087 and will be released there on publication.

References

1. Aharoni-Simon M, Ben-Yaakov K, Sharvit-Bader M et al (2022) Oxidative stress facilitates exogenous mitochondria internalization and survival in retinal ganglion precursor-like cells. Sci Rep 12:5122
2. Arnold AC, Hepler RS, Lieber M, Alexander JM (1996) Hyperbaric oxygen therapy for nonarteritic anterior ischemic optic neuropathy. Am J Ophthalmol 122(4):535–541
3. Avery RL, Bakri SJ, Blumenkranz MS et al (2014) Intravitreal injection technique and monitoring: updated guidelines of an expert panel. Retina 34(Suppl 12):S1–S18
4. Ayupov T, Moreno-Juan V, Curtoni S et al (2026) Cell-type-targeted mitochondrial transplantation rescues cell degeneration. Nature 653:221–231
5. Brestoff JR, Singh KK, Aquilano K et al (2025) Recommendations for mitochondria transfer and transplantation nomenclature and characterization. Nat Metab 7(1):53–67
6. Cakir B, Yeh TC, Lin CH et al (2026) Mitochondrial transplantation in the eye: a review and evaluation of surgical approaches. bioRxiv. 10.64898/2026.04.06.716722. Preprint
7. Chen JW, Gombart ZJ, Rogers S, Gardiner SK, Cecil S, Bullock RM (2011) Pupillary reactivity as an early indicator of increased intracranial pressure: the introduction of the Neurological Pupil index. Surg Neurol Int 2:82
8. Cowan DB, Yao R, Thedsanamoorthy JK, Zurakowski D, Del Nido PJ, McCully JD (2017) Transit and integration of extracellular mitochondria in human heart cells. Sci Rep 7(1):17450
9. Cui Q, Ren C, Sollars PJ, Pickard GE, So KF (2015) The injury resistant ability of melanopsin-expressing intrinsically photosensitive retinal ganglion cells. Neuroscience 284:845–853

10. Doulamis IP, McCully JD (2021) Mitochondrial transplantation for ischemia reperfusion injury. Methods Mol Biol 2277:15–37
11. Durand ML (2017) Bacterial and fungal endophthalmitis. Clin Microbiol Rev 30(3):597–613
12. Emani SM, Piekarski BL, Harrild D, del Nido PJ, McCully JD (2017) Autologous mitochondrial transplantation for dysfunction after ischemia-reperfusion injury. J Thorac Cardiovasc Surg 154(1):286–289
13. Endophthalmitis Vitrectomy Study Group (1995) Results of the Endophthalmitis Vitrectomy Study: a randomized trial of immediate vitrectomy and of intravenous antibiotics for the treatment of postoperative bacterial endophthalmitis. Arch Ophthalmol 113(12):1479–1496
14. Gagnier JJ, Kienle G, Altman DG, Moher D, Sox H, Riley D, CARE Group (2014) The CARE guidelines: consensus-based clinical case report guideline development. J Clin Epidemiol 67(1):46–51
15. Guariento A, Piekarski BL, Doulamis IP et al (2021) Autologous mitochondrial transplantation for cardiogenic shock in pediatric patients following ischemia-reperfusion injury. J Thorac Cardiovasc Surg 162(3):992–1001
16. Hariprasad SM, Mieler WF, Holz ER et al (2004) Determination of vitreous, aqueous, and plasma concentration of orally administered voriconazole in humans. Arch Ophthalmol 122(1):42–47
17. Hariprasad SM, Shah GK, Mieler WF et al (2006) Vitreous and aqueous penetration of orally administered moxifloxacin in humans. Arch Ophthalmol 124(2):178–182
18. Hayakawa K, Esposito E, Wang X et al (2016) Transfer of mitochondria from astrocytes to neurons after stroke. Nature 535(7613):551–555
19. Hayreh SS (2004) Posterior ischaemic optic neuropathy: clinical features, pathogenesis, and management. Eye (Lond) 18(11):1188–1206
20. Hayreh SS (2011) Management of ischemic optic neuropathies. Indian J Ophthalmol 59(2):123–136
21. Ischemic Optic Neuropathy Decompression Trial Research Group (1995) Optic nerve decompression surgery for nonarteritic anterior ischemic optic neuropathy (NAION) is not effective and may be harmful. JAMA 273(8):625–632
22. Lafuente MP, Villegas-Perez MP, Selles-Navarro I, Mayor-Torroglosa S, Miralles de Imperial J, Vidal-Sanz M (2002) Retinal ganglion cell death after acute retinal ischemia is an ongoing process whose severity and duration depends on the duration of the insult. Neuroscience 109(1):157–168
23. McCully JD, Cowan DB, Pacak CA, Toumpoulis IK, Dayalan H, Levitsky S (2009) Injection of isolated mitochondria during early reperfusion for cardioprotection. Am J Physiol Heart Circ Physiol 296(1):H94–H105
24. McCully JD, del Nido PJ, Emani SM (2023) Mitochondrial transplantation: the advance to therapeutic application and molecular modulation. Front Cardiovasc Med 10:1268814
25. Muench NA, Patel S, Maes ME, Donahue RJ, Ikeda A, Nickells RW (2021) The influence of mitochondrial dynamics and function on retinal ganglion cell susceptibility in optic nerve disease. Cells 10(7):1593

26. Nascimento-Dos-Santos G, de-Souza-Ferreira E, Lani R et al (2020) Neuroprotection from optic nerve injury and modulation of oxidative metabolism by transplantation of active mitochondria to the retina. Biochim Biophys Acta Mol Basis Dis 1866(5):165686
27. National Institute for Health and Care Excellence NPi-200 for pupillary light reflex in critical care patients. Medtech innovation briefing MIB235. London: NICE; 12 November 2020. https://www.nice.org.uk/advice/mib235
28. Noh SE, Lee SJ, Cho CS et al (2024) Mitochondrial transplantation attenuates oligomeric amyloid-beta-induced mitochondrial dysfunction and tight junction protein destruction in retinal pigment epithelium. Free Radic Biol Med 212:10–21
29. Oddo M, Taccone FS, Petrosino M et al (2023) ORANGE study investigators. The Neurological Pupil index for outcome prognostication in people with acute brain injury (ORANGE): a prospective, observational, multicentre cohort study. Lancet Neurol 22(10):925–933
30. Ou Y, Jo RE, Ullian EM, Wong ROL, Della Santina L (2016) Selective vulnerability of specific retinal ganglion cell types and synapses after transient ocular hypertension. J Neurosci 36(35):9240–9252
31. Pacak CA, Preble JM, Kondo H et al (2015) Actin-dependent mitochondrial internalization in cardiomyocytes: evidence for rescue of mitochondrial function. Biol Open 4(5):622–626
32. Preble JM, Pacak CA, Kondo H, MacKay AA, Cowan DB, McCully JD (2014) Rapid isolation and purification of mitochondria for transplantation by tissue dissociation and differential filtration. J Vis Exp. ;(91):e51682
33. Ramirez-Barbieri G, Moskowitzova K, Shin B et al (2019) Alloreactivity and allorecognition of syngeneic and allogeneic mitochondria. Mitochondrion 46:103–115
34. Rukmini AV, Milea D, Gooley JJ (2019) Chromatic pupillometry methods for assessing photoreceptor health in retinal and optic nerve diseases. Front Neurol 10:76
35. Selles-Navarro I, Villegas-Perez MP, Salvador-Silva M, Ruiz-Gomez JM, Vidal-Sanz M (1996) Retinal ganglion cell death after different transient periods of pressure-induced ischemia and survival intervals: a quantitative in vivo study. Invest Ophthalmol Vis Sci 37(10):2002–2014
36. Shoyombo I, Aiyagari V, Stutzman SE et al (2018) Understanding the relationship between the Neurologic Pupil index and constriction velocity values. Sci Rep 8(1):6992
37. Tao X, Sabharwal J, Seilheimer RL, Wu SM, Frankfort BJ (2019) Mild intraocular pressure elevation in mice reveals distinct retinal ganglion cell functional thresholds and pressure-dependent properties. J Neurosci 39(10):1881–1891
38. Tapia ML, Nascimento-Dos-Santos G, Park KK (2022) Subtype-specific survival and regeneration of retinal ganglion cells in response to injury. Front Cell Dev Biol 10:956279
39. Thompson HS, Montague P, Cox TA, Corbett JJ (1982) The relationship between visual acuity, pupillary defect, and visual field loss. Am J Ophthalmol 93(6):681–688
40. US Food and Drug Administration (2026) Chemistry, Manufacturing, and Controls Flexibilities for Developing Human Cellular and Gene Therapy Products for a Biologics License Application. Guidance for Industry. FDA; May, Silver Spring, MD

41. Walker M, Levitt MR, Federico EM et al (2026) Autologous mitochondrial transplant for acute cerebral ischemia: phase 1 trial results and review. J Cereb Blood Flow Metab 46(2):322–332
42. Wang Y, Liu N, Hu L et al (2024) Nanoengineered mitochondria enable ocular mitochondrial disease therapy via the replacement of dysfunctional mitochondria. Acta Pharm Sin B 14(12):5435–5450
43. Wu SF, Lin CY, Tsai RK et al (2022) Mitochondrial transplantation moderately ameliorates retinal degeneration in Royal College of Surgeons rats. Biomedicines 10(11):2883
44. Yoshida T, Yokoi T, Tanaka T et al (2024) Modeling of retina and optic nerve ischemia-reperfusion injury through hypoxia-reoxygenation in human induced pluripotent stem cell-derived retinal ganglion cells. Cells 13(2):130
45. You W, Knoops K, Boesten I et al (2024) A time window for rescuing dying retinal ganglion cells. Cell Commun Signal 22:88

Figures

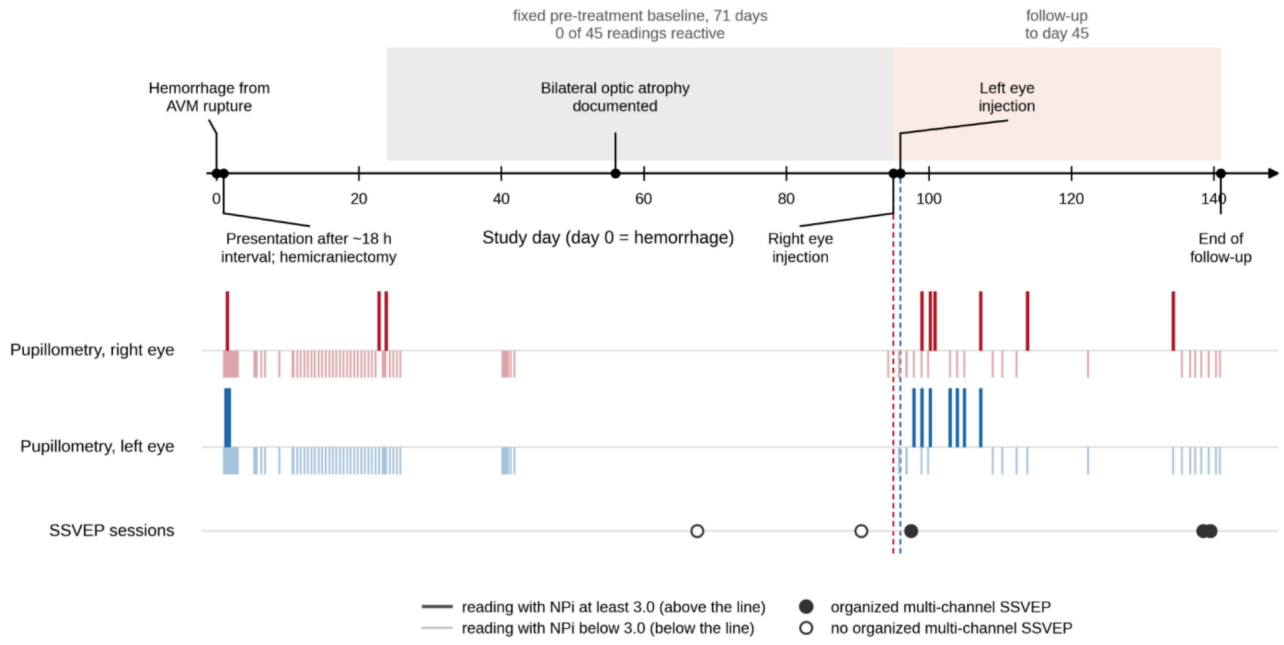


Figure 1

Timeline of injury, treatment and assessment. Events from rupture of the arteriovenous malformation through the end of follow-up, on a study-day axis with day 0 at the hemorrhage. Marked events are the estimated 18-hour pre-hospital interval and decompressive hemicraniectomy with clot evacuation, the neuro-ophthalmological examination at 8 weeks documenting bilateral optic disc pallor and atrophy, the two intravitreal procedures 24 hours apart, and the end of follow-up. Each tick on the lower rows is one pupillometry reading. Readings meeting the criterion for a normal light reaction (Neurological Pupil index

at least 3.0) are drawn as long ticks above each row line and readings below the criterion as short ticks below it, so that a dense cluster of non-reactive readings cannot be mistaken for a reactive one; circles mark steady-state visual evoked potential sessions, filled where an organized multi-channel occipital response was present. The shaded block is the 71-day fixed baseline immediately preceding treatment, during which 45 readings were obtained across both eyes and none met the criterion. The interval between study days 43 and 95 contains no pupillometry readings.

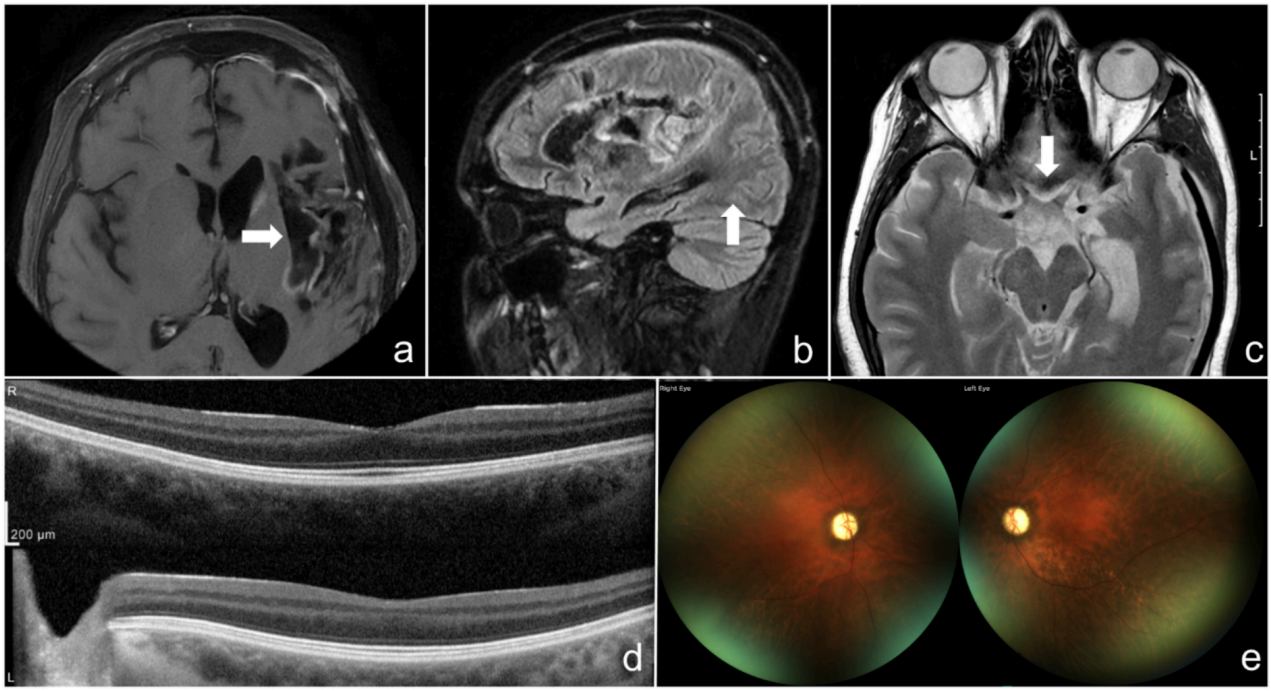


Figure 2

Structural imaging at the time of treatment. a, Axial magnetic resonance imaging (MRI) showing the mature left frontal postoperative cavity (fluid-attenuated inversion recovery, FLAIR; arrow). b, Sagittal MRI showing intact occipital cortex without ischemic injury (FLAIR; arrow). c, Axial MRI showing volume loss of the optic chiasm and prechiasmatic optic nerves without active T2 signal change (arrow). d, Optical coherence tomography of each eye showing normal outer retinal and foveal morphology with severe thinning of the nerve fiber layer and ganglion cell layer; single acquisitions, serial imaging with normative comparison could not be obtained. e, Fundus photographs obtained with a RetCam in the operating room before the first injection, showing optic disc pallor in both eyes.

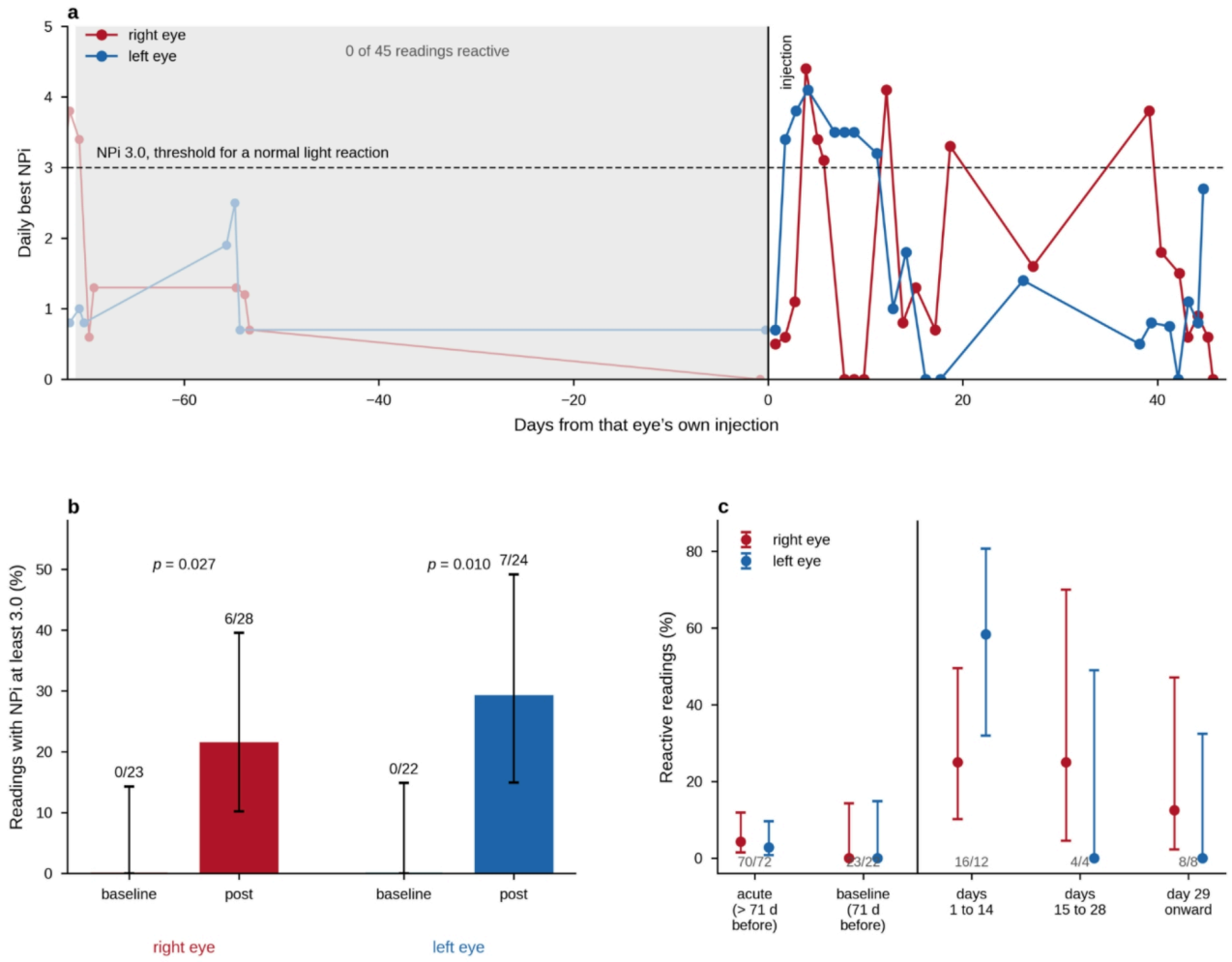


Figure 3

Pupillary reactivity before and after treatment. a, Daily best Neurological Pupil index for each eye against time from that eye's own procedure. The shaded block is the 71-day fixed baseline; the dashed horizontal line is the criterion for a normal light reaction. b, Proportion of readings meeting the criterion in the fixed baseline and after treatment, by eye, with Wilson 95 percent intervals and Fisher exact p values; numerators and denominators are shown above each bar. c, Reactive rate by epoch with Wilson 95 percent intervals; grey figures below each epoch give the number of readings in the right and left eyes. Denominators in the later epochs are small.

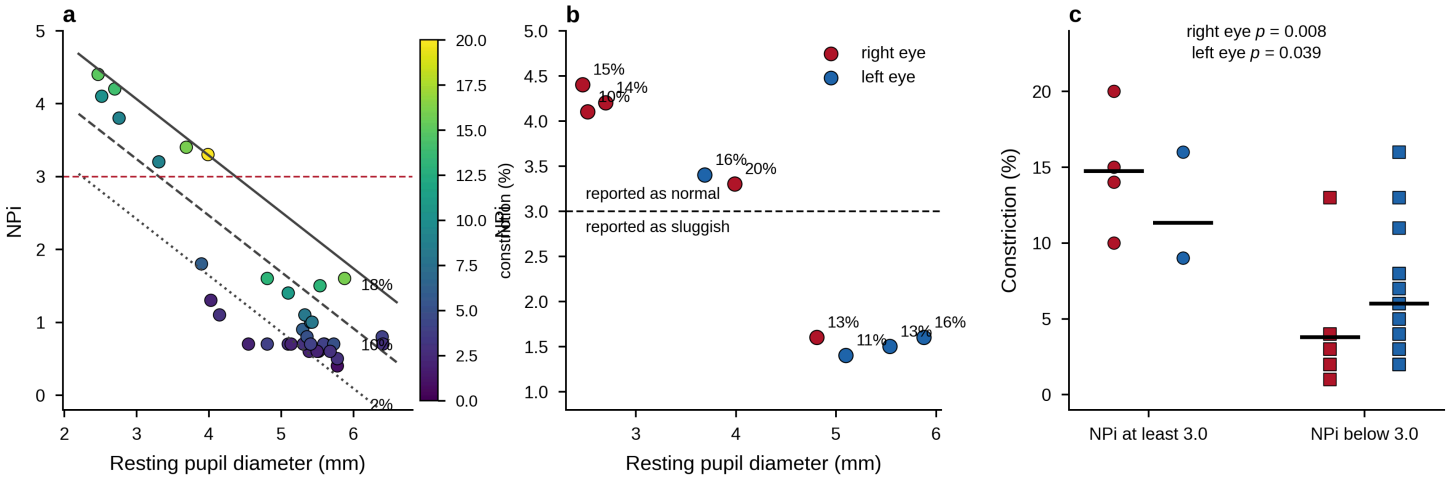


Figure 4

The pupillometry index is dominated by resting pupil diameter. a, Neurological Pupil index against resting pupil diameter for the 36 of 40 device captures with a complete component vector, colored by percentage constriction. Lines are the fitted two-term model at 2, 10 and 18 percent constriction; the dashed horizontal line is the criterion for a normal light reaction. b, The 9 captures meeting an independent criterion for a measured reflex, defined as constriction of at least 10 percent, labeled with their constriction values. Captures with equal or greater constriction are reported as normal at small resting diameters and as sluggish at large ones. c, Percentage constriction in captures above and below the index criterion, by eye, with group means; p values are Mann-Whitney. Component data are available only from the treatment period onward.

Supplementary Files

This is a list of supplementary files associated with this preprint. Click to download.

- SupplementaryInformation.pdf